Technetium(VII) Dioxotrifluoride, TcO_2F_3: Synthesis, X-ray Structure Determination, and Raman Spectrum†

Hélène P. A. Mercier and Gary J. Schrobilgen*

Department of Chemistry, McMaster University, Hamilton, Ontario L8S 4M1, Canada

Received July 30, 1992

The synthesis of TcO_2F_3, which is reported for the first time, was accomplished by the reaction of XeF_6 and Tc_2O_7 in a 3:1 molar ratio in anhydrous HF solution. Technetium(VII) dioxotrifluoride is yellow (mp 200 ± 1 °C) and crystallized in the triclinic system, space group $P\bar{1}$, with a = 7.774 (3) Å, b = 7.797 (1) Å, c = 11.602 (3) Å, α = 89.41 (2)°, β = 88.63 (3)°, γ = 84.32 (2)°, V = 699.6 (3) Å^3, D_{calc} = 3.551 g cm^{-3} for Z = 8 from HF solutions containing excess XeF_6. The structure consists of open chains of fluorine bridged TcO_2F_4 units in which the bridge fluorines (F_b) are trans to the oxygens and the light atoms surrounding technetium form near-undistorted octahedra in which the technetium atoms are displaced toward the oxygen atom in the [F_b,F_b,O,O] plane: terminal Tc–F, 1.834 (7) Å; bridging Tc- - -F, 2.080 (5) Å; Tc–O, 1.646 (9) Å; Tc- - -F- - -Tc, 148.8 (3)°. The Raman spectrum of the polymeric *cis*-TcO_2F_4 unit has been assigned under C_{2v} point symmetry and exhibits only weak vibrational coupling in the unit cell.

Introduction

The fluoride and oxofluoride chemistry of technetium represents all the common oxidation states of technetium, but is limited to TcF_6^{2-},[1] TcF_5,[2] TcF_6^-,[2,3] TcF_6,[4] TcF_7^-,[3] TcF_8^{2-},[3] $TcOF_4$[2,5] and TcO_3F.[6] Although ReO_2F_3[8-10] is known and is well characterized by matrix-isolation vibrational spectroscopy, the technetium(VII) analog, TcO_2F_3, has not been isolated and characterized. The recent observation of the $TcO_2F_2^+$ cation in a mass spectrometry study of the products resulting from the high-temperature reaction of partially oxidized technetium metal with fluorine has provided indirect evidence for the formation of TcO_2F_3.[11] Moreover, there is an overall paucity of detailed X-ray structural data for the dioxotrifluorides of group 7 as well as other known technetium fluoride and oxofluoride species: $TcOF_4$[5] is the only fluoro species to have been characterized crystallographically, while only unit cell parameters are available for TcF_5.[2]

Pertechnetyl fluoride, TcO_3F, is the only oxofluoride of technetium(VII) that has been reported and unambiguously characterized to date, and it has been prepared as a pure compound by reaction of TcO_2 with F_2 mixtures in a flow system.[6a] This result is surprising in view of a previous report that ReO_2F_3 and $ReOF_5$ are the major products in the reaction of fluorine with ReO_2[8] and seems to be at variance with a recent mass spectrometry study of the products of the high-temperature reaction of Tc/TcO_2 with F_2.[11] It also has been shown that the solvolysis of TcO_4^- in anhydrous HF leads to TcO_3F.[6b] The solvolysis of oxides in anhydrous HF is an established method for the synthesis of fluorides and oxofluorides.[12] However, if a desired product is readily hydrolyzed by water formed as a byproduct, more highly fluorinated oxofluorides are unlikely to form. A preliminary ^{99}Tc and ^{19}F NMR study from this laboratory indicated that higher fluorinated oxofluorides of Tc(VII) are formed when anhydrous HF solutions of TcO_4^-, consisting of TcO_3F and water tied up as H_3O^+, are treated with either KrF_2 or XeF_6.[13] Both reagents serve to remove water from the solvent medium by redox elimination of O_2/Kr and O_2/XeF_4 or by oxide/fluoride metathesis with XeF_6 to give HF and $XeOF_4$. The present work is an extension of the previous NMR study and describes the synthesis and structural characterization of the second known oxofluoride of Tc(VII), TcO_2F_3, and first complete structural characterization of a technetium(VII) oxofluoride by X-ray crystallography.

Results and Discussion

Synthesis of TcO_2F_3. Technetium heptoxide, Tc_2O_7, is sparingly soluble in anhydrous HF at room temperature to yield a two-phase system consisting of a very pale yellow solution in HF and a lower layer consisting of a yellow liquid. It has been previously shown that $NH_4^+TcO_4^-$ undergoes solvolysis in HF, yielding TcO_3F, and forms a similar bilayer system.[6b] The ^{99}Tc NMR spectra of both layers were recorded in the present study and shown to contain TcO_3F [δ(^{99}Tc), 44.6 ppm)],[13] and this is consistent with the formation of TcO_3F according to eq 1. The

$$Tc_2O_7 + 4HF \rightarrow 2TcO_3F + H_3O^+ + HF_2^- \qquad (1)$$

addition of XeF_6 to these solutions results in the formation of TcO_2F_3 and can be viewed as a two-step process: (1) the addition of XeF_6 to solutions of H_2O in HF leading to the formation of $XeOF_4$ according to eq 2, a well-established route for the generation of $XeOF_4$ in HF solution,[14] and (2) the fluorination of TcO_3F by XeF_6 to give TcO_2F_3 by fluorine/oxygen metathesis (eq 3) and competing redox reactions which yield XeF_2 and O_2 (eqs 4 and 5). The reaction of XeF_6 with Tc_2O_7 resulted in a microcrystalline precipitate of TcO_2F_3. The ^{129}Xe NMR of the resulting supernatants showed an intense quintet arising from $XeOF_4$ (δ(^{129}Xe), 22.7 ppm; ^1J(^{129}Xe–^{19}F), 1128 Hz) and a weak triplet arising from XeF_2 (δ(^{129}Xe), −1587 ppm; ^1J(^{129}Xe–^{19}F), 5679 Hz). The formation of $XeOF_4$ is in accord with eqs 2 and 3, whereas the weak resonance arising from XeF_2 likely arises from further reaction of $XeOF_4$ with water (eq 4) or TcO_3F (eq 5) to form XeO_2F_2, which slowly decomposes in HF at room temperature to form XeF_2 and O_2 (eq 6). We have previously

† Dedicated to Professor Friedhelm Aubke on the occasion of his 60th birthday.

(1) Schwochau, K.; Herr, W. *Angew. Chem., Int. Ed. Engl.* **1963**, *2*, 97.
(2) Hugill, D.; Edwards, A. J.; Peacock, R. D. *Nature* **1963**, *200*, 672.
(3) Holloway, J. H.; Selig, H. *J. Inorg. Nucl. Chem.* **1968**, *30*, 473.
(4) Selig, H.; Chernick, C. L.; Malm, J. G. *J. Inorg. Nucl. Chem.* **1961**, *19*, 377.
(5) Edwards, A. J.; Jones, G. R.; Sills, R. J. C. *J. Chem. Soc. A* **1970**, 2521.
(6) (a) Selig, H.; Malm, J. G. *J. Inorg. Nucl. Chem.* **1963**, *25*, 349. (b) Binenboym, J.; El-Gad, U.; Selig, H. *Inorg. Chem.* **1974**, *13*, 319.
(7) Beattie, I. R.; Crocombe, R. A.; Ogden, J. S. *J. Chem. Soc., Dalton Trans.* **1977**, 1481.
(8) Aynsley, E. E.; Peacock, R. D.; Robinson, P. L. *J. Chem. Soc.* **1950**, 1622.
(9) Cady, G. H.; Hargreaves, G. B. *J. Inorg. Nucl. Chem.* **1957**, *4*, 24.
(10) Sunder, W. A.; Stevie, F. A. *J. Fluorine Chem.* **1975**, *6*, 449.
(11) Gibson, J. K. *J. Fluorine Chem.* **1991**, *55*, 299.
(12) Muetterties, E. L.; Tullock, C. W. *Prep. Inorg. React.* **1965**, *2*, 270.
(13) Franklin, K. J.; Lock, C. J. L.; Sayer, B. G.; Schrobilgen, G. J. *J. Am. Chem. Soc.* **1982**, *104*, 5303.
(14) Gillespie, R. J.; Schrobilgen, G. J. *Inorg. Chem.* **1974**, *13*, 2370.

0020-1669/93/1332-0145$04.00/0

$$XeF_6 + H_3O^+ + HF_2^- \rightarrow XeOF_4 + 4HF \quad (2)$$

$$XeF_6 + TcO_3F \rightarrow TcO_2F_3 + XeOF_4 \quad (3)$$

$$XeOF_4 + H_3O^+ + HF_2^- \rightarrow XeO_2F_2 + 4HF \quad (4)$$

$$XeOF_4 + TcO_3F \rightarrow TcO_2F_3 + XeO_2F_2 \quad (5)$$

$$XeO_2F_2 \rightarrow XeF_2 + O_2 \quad (6)$$

$$XeF_6 + TcO_3F \rightarrow TcO_2F_3 + XeF_4 + {}^1/_2O_2 \quad (7)$$

$$TcO_3F + XeF_4 \longrightarrow TcO_2F_3 + [O{=}XeF_2] \quad (8)$$

$$[O{=}XeF_2] \rightarrow XeF_2 + {}^1/_2O_2$$

shown that HF solutions of $K^+TcO_4^-$ react with XeF_6 to give rise to significant amounts of XeF_4 and a new technetium(VII) oxofluoro species[13] now assigned to the $TcO_2F_4^-$ anion (vide infra). It is unlikely that XeF_2 observed in the present system arises from the redox reactions (7) and (8). Were XeF_4 to form, its lower reactivity relative to that of XeF_6, which is in excess, is inconsistent with our failure to observe XeF_4 in the NMR spectra.

Pure TcO_2F_3 is lemon yellow in color with a melting point of 200 ± 1 °C and is essentially insoluble in anhydrous HF at room temperature. Addition of excess XeF_6 to TcO_2F_3 in HF results in dissolution to give a yellow solution. Xenon hexafluoride presumably acts as a fluoride ion donor[15] toward TcO_2F_3 to give equilibrium concentrations of the HF-soluble salt $XeF_5^+TcO_2F_4^-$ (eq 9) and accounts for the fact that, despite the insolubility of

$$XeF_6 + TcO_2F_3 \rightleftharpoons XeF_5^+TcO_2F_4^- \quad (9)$$

TcO_2F_3 in anhydrous HF, single crystals of TcO_2F_3 could nevertheless be grown from HF solution by slow cooling of warmed solutions in which $XeF_5^+TcO_2F_4^-$ formation is favored, i.e., at a molar ratio of XeF_6:Tc_2O_7 = 5:1 (eqs 1–4 and eq 9; also see Experimental Section). The ^{129}Xe NMR spectra of the supernatants in which XeF_6 is in excess relative to the ideal 3:1 stoichiometry needed for quantitative conversion of Tc_2O_7 to TcO_2F_3 also show resonances between 0 and 6 ppm attributed to XeF_6 and XeF_5^+ undergoing rapid fluorine exchange. The NMR spectra of the supernatants also reveal a broad triplet in the ^{99}Tc spectrum [258.2 ppm; $^1J(^{99}Tc-^{19}F)$, 259 Hz] and a broad partially quadrupole collapsed decet in the ^{19}F spectrum at 20.8 ppm (saddle-shaped resonance with the two outer lines being clearly resolved with a peak to peak separation of 2140 Hz). We have previously shown that these ^{19}F and ^{99}Tc resonances are also associated with the $K^+TcO_4^-/XeF_6$ and $K^+TcO_4^-/KrF_2$ systems in HF solvent.[13] The multiplets are assigned to the *cis*-$TcO_2F_4^-$ anion in which the longer Tc–F bonds trans to the oxygens (cf. *cis*-TcO_2F_4 unit in TcO_2F_3) are presumed to be labile and undergo fluorine exchange with HF solvent, whereas the shorter axial Tc–F bonds are nonlabile and spin–spin couple to ^{99}Tc.[16]

X-ray Crystal Structure of TcO_2F_3. Details of the data collection parameters and other crystallographic information for the $P\bar{1}$ space group are given in Table I. The final atomic coordinates and the equivalent isotropic thermal parameters are summarized in Table II. Important bond lengths, angles, and significant long contacts for the four TcO_2F_3 crystallographically independent units, which had to be defined in the $P\bar{1}$ space group, are listed in Table III. Figures 1 and 2 show the asymmetric unit of the crystal structure and a view of the local environment around one of the technetium atoms.

Table I. Summary of Crystal Data and Refinement Resutls for TcO_2F_3

space group	$P\bar{1}$ (No. 2)	molecules/unit cell	8
a (Å)	7.774 (3)	mol wt (g mol^{-1})	187.0
b (Å)	7.797 (1)	calcd density (g cm^{-3})	3.551
c (Å)	11.602 (3)	T (°C)	−100
α (deg)	89.41 (2)	μ (mm^{-1})	4.048
β (deg)	88.63 (3)	wavelength (Å) used	0.56086
γ (deg)	84.32 (2)	for data collection	
V (Å^3)	699.6 (3)	final agreement factors	R = 0.042; R_w = 0.043

Table II. Atomic Coordinates (×10^4) and Equivalent Isotropic Displacement Coefficients (Å^2 × 10^3) in TcO_2F_3

	x	y	z	U(eq)[a]
F(1)	0	0	0	54 (4)
Tc(1)	2172 (1)	482 (1)	−957 (1)	30 (1)
F(2)	493 (9)	1693 (8)	−1821 (6)	46 (2)
F(3)	3203 (9)	−341 (8)	368 (5)	38 (2)
O(1)	2157 (14)	−1345 (11)	−1617 (8)	57 (3)
O(2)	3830 (13)	1342 (13)	−1545 (8)	55 (3)
F(4)	1699 (10)	2697 (7)	39 (6)	44 (2)
Tc(2)	2464 (1)	4478 (1)	1207 (1)	29 (1)
F(5)	207 (9)	4421 (8)	1682 (6)	44 (2)
F(6)	4612 (9)	3533 (8)	686 (6)	45 (2)
O(3)	2145 (12)	5990 (9)	207 (7)	43 (3)
O(4)	3124 (13)	5544 (10)	2301 (8)	52 (3)
F(7)	2762 (9)	2245 (7)	2204 (5)	38 (2)
Tc(3)	2494 (1)	829 (1)	3707 (1)	28 (1)
F(8)	210 (9)	1543 (9)	3431 (6)	45 (2)
F(9)	4814 (9)	1086 (8)	3765 (7)	45 (2)
O(5)	2650 (11)	−980 (9)	2964 (7)	41 (3)
O(6)	2210 (12)	167 (11)	5053 (7)	45 (3)
F(10)	2378 (9)	3364 (7)	4333 (5)	37 (2)
Tc(4)	2716 (1)	4704 (1)	5859 (1)	30 (1)
F(11)	2031 (10)	6500 (8)	4920 (7)	50 (2)
F(12)	3895 (11)	2630 (9)	6229 (6)	59 (3)
O(7)	789 (12)	4216 (14)	6279 (8)	57 (3)
O(8)	3326 (12)	5777 (11)	6973 (8)	51 (3)
F(13)	5000	5000	5000	65 (5)

[a] Equivalent isotropic U defined as one-third of the trace of the orthogonalized U_{ij} tensor.

The structure of TcO_2F_3 consists of open chains of molecules parallel to the *b*-axis of the unit cell. The technetium atoms form a "zigzag" chain linked symmetrically by cis-bridging fluorine atoms, with two fluorines and two terminal oxygen atoms completing a distorted octahedral arrangement (Figure 1). The structure is consequently closely related to those of $MoOF_4$[17] and $ReOF_4$,[18] which also consist of infinite chains of cis-fluorine-bridged oxotetrafluoride units in which the oxygen atoms are trans to the fluorine bridges with two trans-terminal fluorines completing the distorted octahedral coordination around the technetium atoms. The pseudooctahedral coordination around the technetium atom is remarkably similar to that of tungsten in WO_2F_2·bpy in which the ligand nitrogen atoms of 2,2′-bipyridyl occur trans to the W=O bonds.[19] The metal atoms in the related polymeric oxotetrafluorides of molybdenum,[17] tungsten,[20] technetium,[5] and rhenium[18] and the transition-metal binary fluorides[21] are also coordinated to an octahedron of light atoms. The structural unit of TcO_2F_3 consists of four such crystallographically distinct pseudooctahedra in which the bond lengths and angles are the same within the experimental errors (Table III). The bond lengths fall into three groups: (a) 1.834 (7) Å, the terminal

(15) Selig, H.; Holloway, J. H. *Top. Curr. Chem.* **1984**, *124*, 33.
(16) Casteel, W. M.; LeBlond, N.; Mercier, H. A. P.; Schrobilgen, G. J. *Inorg. Chem.*, to be submitted for publication.
(17) Edwards, A. J.; Steventon, B. R. *J. Chem. Soc. A* **1968**, 2503.
(18) Edwards, A. J.; Jones, G. R. *J. Chem. Soc. A* **1968**, 2511.
(19) Arnaudet, L.; Bougon, R.; Ban, B.; Charpin, P.; Isabey, J.; Lance, M.; Nierlich, M.; Vigner, J. *Can. J. Chem.* **1990**, *68*, 507.
(20) Edwards, A. J.; Jones, G. R. *J. Chem. Soc. A* **1968**, 2074. Although bridging oxygens were originally reported for the tetrameric unit of the WOF_4 structure, it is now clear that the anomalously short terminal W–F bonds observed in this structure must be attributed to terminal W=O bonds and that the structure is actually fluorine bridged.

Table III. Bond Lengths (Å), Bond Valences (vu) and Bond Angles (deg) in TcO_2F_3

Bond Lengths (Å) and Corresponding Bond Valences (vu)[a]

	Tc(1)–F(1)	Tc(1)–F(2)	Tc(1)–F(3)	Tc(1)–F(4)	Tc(1)–O(1)	Tc(1)–O(2)
bond valence	0.534	0.963	0.995	0.502	2.047	1.949
bond length	2.062 (1)	1.844 (7)	1.832 (6)	2.085 (6)	1.625 (9)	1.643 (10)
tot. bond valence: 6.99						
	Tc(2)–F(4)	Tc(2)–F(5)	Tc(2)–F(6)	Tc(2)–F(7)	Tc(2)–O(3)	Tc(2)–O(4)
bond valence	0.498	0.997	0.953	0.512	1.908	1.944
bond length	2.088 (7)	1.831 (7)	1.848 (7)	2.078 (6)	1.651 (8)	1.644 (9)
tot. bond valence: 6.81						
	Tc(3)–F(7)	Tc(3)–F(8)	Tc(3)–F(9)	Tc(3)–F(10)	Tc(3)–O(5)	Tc(3)–O(6)
bond valence	0.521	0.968	0.981	0.474	1.898	1.877
bond length	2.071 (6)	1.842 (7)	1.837 (7)	2.106 (6)	1.653 (7)	1.657 (8)
tot. bond valence: 6.72						
	Tc(4)–F(10)	Tc(4)–F(11)	Tc(4)–F(12)	Tc(4)–F(13)	Tc(4)–O(7)	Tc(4)–O(8)
bond valence	0.482	1.053	1.001	0.555	1.949	1.908
bond length	2.100 (6)	1.811 (7)	1.830 (7)	2.048 (1)	1.643 (10)	1.651 (9)
tot. bond valence: 6.95						

Bond Angles (deg)

F(1)–Tc(1)–F(2)	80.2 (2)	F(4)–Tc(2)–F(5)	80.3 (3)	F(7)–Tc(3)–F(8)	79.7 (3)	F(10)–Tc(4)–F(11)	80.3 (3)
F(1)–Tc(1)–F(3)	80.6 (2)	F(4)–Tc(2)–F(6)	80.5 (3)	F(7)–Tc(3)–F(9)	80.9 (3)	F(10)–Tc(4)–F(12)	80.7 (3)
F(1)–Tc(1)–O(1)	90.7 (4)	F(5)–Tc(2)–F(6)	155.0 (3)	F(8)–Tc(3)–F(9)	154.9 (3)	F(11)–Tc(4)–F(12)	155.3 (3)
F(3)–Tc(1)–O(1)	98.1 (4)	F(4)–Tc(2)–O(3)	88.8 (3)	F(7)–Tc(3)–O(5)	90.7 (3)	F(10)–Tc(4)–O(7)	87.4 (4)
F(2)–Tc(1)–O(2)	96.7 (4)	F(5)–Tc(2)–O(3)	97.7 (4)	F(8)–Tc(3)–O(5)	98.2 (4)	F(11)–Tc(4)–O(7)	97.9 (4)
O(1)–Tc(1)–O(2)	104.1 (5)	F(6)–Tc(2)–O(3)	97.7 (4)	F(9)–Tc(3)–O(5)	97.8 (4)	F(12)–Tc(4)–O(7)	96.9 (4)
F(2)–Tc(1)–F(4)	80.1 (3)	F(4)–Tc(2)–O(4)	168.5 (3)	F(7)–Tc(3)–O(6)	166.0 (3)	F(10)–Tc(4)–O(8)	170.1 (4)
O(1)–Tc(1)–F(4)	168.0 (4)	F(5)–Tc(2)–O(4)	98.1 (4)	F(8)–Tc(3)–O(6)	97.0 (4)	F(11)–Tc(4)–O(8)	99.3 (4)
F(2)–Tc(1)–F(3)	155.9 (3)	F(6)–Tc(2)–O(4)	97.5 (4)	F(9)–Tc(3)–O(6)	98.0 (4)	F(12)–Tc(4)–O(8)	96.6 (4)
F(2)–Tc(1)–O(1)	96.7 (4)	O(3)–Tc(2)–O(4)	102.7 (4)	O(5)–Tc(3)–O(6)	103.3 (4)	O(7)–Tc(4)–O(8)	102.4 (5)
F(1)–Tc(1)–O(2)	165.2 (3)	F(4)–Tc(2)–F(7)	79.8 (2)	F(7)–Tc(3)–F(10)	78.0 (2)	F(10)–Tc(4)–F(13)	79.2 (2)
F(3)–Tc(1)–O(2)	98.1 (4)	F(5)–Tc(2)–F(7)	81.6 (3)	F(8)–Tc(3)–F(10)	80.4 (3)	F(11)–Tc(4)–F(13)	79.9 (3)
F(1)–Tc(1)–F(4)	77.4 (2)	F(6)–Tc(2)–F(7)	79.3 (3)	F(9)–Tc(3)–F(10)	80.1 (3)	F(12)–Tc(4)–F(13)	81.1 (3)
F(3)–Tc(1)–F(4)	81.5 (3)	O(3)–Tc(2)–F(7)	168.5 (3)	O(5)–Tc(3)–F(10)	168.6 (3)	O(7)–Tc(4)–F(13)	166.6 (4)
O(2)–Tc(1)–F(4)	87.8 (4)	O(4)–Tc(2)–F(7)	88.7 (3)	O(6)–Tc(3)–F(10)	88.1 (3)	O(8)–Tc(4)–F(13)	90.9 (3)
Tc(1)–F(4)–Tc(2)	152.0 (4)	Tc(2)–F(7)–Tc(3)	153.8 (3)	Tc(3)–F(10)–Tc(4)	140.5 (3)		

[a] Bond valence units (v.u.) are defined in refs 24–26. R_0 = 1.83 (Tc=O), R_0 = 1.89 (Tc–F) and B = 0.37 were used; Brown, I. D. Department of Physics, McMaster University, Hamilton, Ontario L8S 4M1, Canada. Private communication.

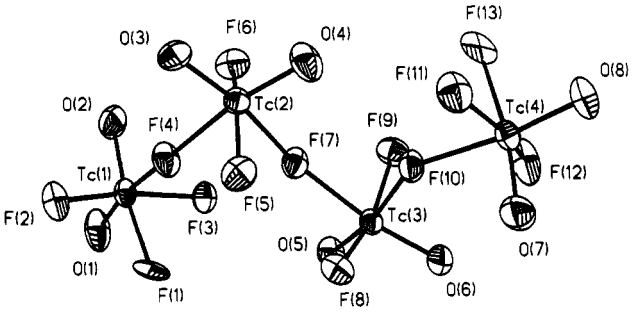

Figure 1. Asymmetric unit of the crystal structure of TcO_2F_3 showing the numbering of the atoms; thermal ellipsoids are shown at the 50% probability level.

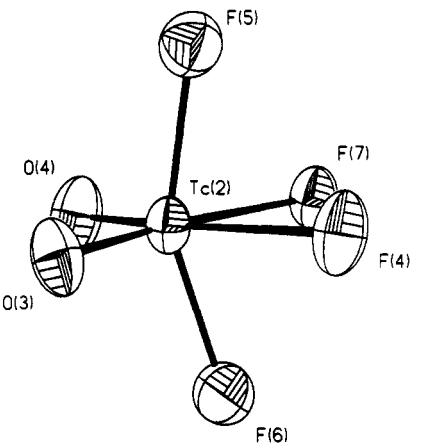

Figure 2. Local environment around technetium in TcO_2F_3 showing that the technetium is displaced toward the oxygen atoms; only the Tc(2) environment is depicted.

Tc–F distances; (b) 1.646 (9) Å, the Tc–O distances; and (c) 2.080 (5) Å, the Tc–F bridging fluorine distances. The two long bridge bond lengths are opposite to the two oxygen atoms. The distance 1.646 (9) Å is characteristic of a Tc–O double bond even though it is slightly smaller than the terminal Tc–O bond length found in the starting material, Tc_2O_7 (1.672 (8) Å),[22] as well as in TcO_4^- in $N(CH_3)_4^+TcO_4^-$ (1.676 (8) Å)[23] and in the trimer $(TcOF_4)_3$ (1.66 (3) Å)[5] where the technetium is in its +6 oxidation state. Little or no information is available in the literature regarding Tc–F bond distances, there are no Tc(VII)–F distances known, and only Tc(VI)–F distances have been determined in $(TcOF_4)_3$.[5] The Tc–F terminal bond in TcO_2F_3 (1.834 (7) Å) is in good agreement with the terminal Tc–F bond distance in $(TcOF_4)_3$ (1.81 (3) Å), while the Tc–F bridging bonds (mean 2.080 (5) Å) are found to be intermediate between the two Tc–F bridging bonds in $(TcOF_4)_3$ (2.26 (2) and 1.89 (2) Å). The bond valences for individual bonds as defined by Brown[24–26] are included in Table III. Taking into account the two fluorine bridge contacts,

(21) (a) Edwards, A. J. *Adv. Inorg. Radiochem.* **1983**, *27*, 83. (b) Babel, D.; Tressaud, A. In *Inorganic Solid Fluorides*; Hagenmüller, P., Ed.; Academic Press, Inc.: New York, 1985; pp 78–204. (c) Müller, B. G. *Angew. Chem., Int. Ed. Engl.* **1987**, *26*, 1081.
(22) Krebs, von B. *Z. Anorg. Allg. Chem.* **1971**, *380*, 146.
(23) German, K. E.; Grigor'ev, M. S.; Kuzina, A. F.; Gulev, B. F.; Spitsyn, V. I. *Dokl. Akad. Nauk SSSR* **1986**, *287*, 650.
(24) Brown, I. D. *J. Solid State Chem.* **1974**, *11*, 214.
(25) Brown, I. D. In *Structure and Bonding in Crystals*; O'Keefe, M., Navrotsky, A., Eds.; Academic Press: London, 1981; Vol. 2, p 1.
(26) Brown, I. D.; Altermatt, D. *Acta Crystallogr.* **1985**, *B41*, 244.

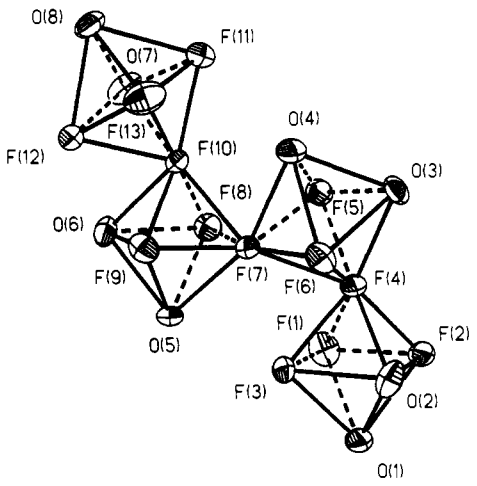

Figure 3. Octahedra formed by the light atoms surrounding the technetium atoms in the structural unit of TcO_2F_3.

the total bond valences for the four technetium atoms range from 6.72 to 6.99 vu (bond valence units), with contributions of 1.88–2.05 vu/oxygen atom, 0.95–1.05 vu/terminal fluorine atom, and 0.47–0.56 vu/bridging fluorine to the total bond valence of each technetium atom. The total bond valences of the technetium and bridging fluorine atoms confirm that only two significant long fluorine bridge contacts need to be taken into account in a description of the structure of TcO_2F_3.

Despite considerable variations in the bond lengths and bond angles around the technetium atoms of TcO_2F_3, the octahedra formed by the light atoms are relatively undistorted having mean F···F_b, F_b···F_b, F···O, F_b···O, and O···O distances of 2.541, 2.636, 2.622, 2.632, and 2.578 Å, respectively. The light atom–light atom distances are given in supplementary Table 7 and the four independent octahedra are shown in Figure 3. The light atom octahedra observed in the structures of $MoOF_4$,[17] WOF_4,[20] $ReOF_4$,[18] and $TcOF_4$[5] are also relatively undistorted, with the packing of light atom octahedra dominating these structures. The close-packing arrangements in these structures have been correlated with the M- - -F- - -M angle, with hexagonal close packing and cubic close packing giving ideal angles of 132 and 180°, respectively. For example, the ideal hexagonal close-packed angle is approached in the open chain structure of monoclinic $ReOF_4$, where Re- - -F- - -Re is 139 (4)°. In contrast, the structure of WOF_4, in which the light atoms are hexagonally close packed, shows a W- - -F- - -W angle of 173 (1)°. The Tc- - -F- - -Tc angle in TcO_2F_3 is 148.8 (3)° and is similar to the Mo- - -F- - -Mo angle of 151.0 (5)° in the open chain structure of monoclinic $MoOF_4$. The bridge angles in TcO_2F_3 and $MoOF_4$ are inconsistent with either close-packed system, but are nearer to the theoretical angle for hexagonal close packing. The interatomic contact distances (supplementary material, Table 7) are all within the range 2.527–3.490 Å, which is consistent with close packing of the light atoms.

The eccentricities of the technetium atoms in the octahedra defined by their ligand atoms are described relative to the three orthogonal planes of each light atom octahedron. The two oxygen atoms, their trans fluorine atoms, and the technetium atom of each *cis*-TcO_2F_4 unit are coplanar, defining a unique plane with maximum deviations from the ideal plane ranging from 0.004 to 0.018 Å. The two [O,F,F,F_b] planes orthogonal to the [O,O,Tc,-F_b,F_b] plane, defined by a single oxygen and three fluorine atoms, do not contain the technetium atom; consequently, the distortion of the octahedral environment around each technetium atom is described as a displacement of 0.216 (5)–0.257 (4) Å of the technetium atom from both [O,F,F,F_b] planes toward the oxygens in the [O,O,Tc,F_b,F_b] plane. This displacement is similar to that observed for the metal atoms in $MoOF_4$ (0.31 Å),[17] WOF_4 (0.30 Å),[20] $ReOF_4$ (0.30 Å),[18] and $TcOF_4$ (0.36 Å).[5]

The greater spatial requirement of each oxygen double bond domain and its repulsive interaction with electron bond pair domains at approximately right angles to it in the [O,F,F,F_b] plane cause the angle subtended by the terminal fluorine atom and oxygen atom of the plane and the second oxygen atom cis to the plane to be significantly greater than 90° (O–Tc–O, 102.4 (5)–104.1 (5)°; O–Tc–F, 96.6 (4)–99.3 (4)°). These distortions are presumably heightened by the smaller spatial requirement of the longer Tc- - -F_b bond domain trans to the oxygen. The smaller angles between the Tc- - -F_b bonds cis to the Tc–O bonds (87.4 (4)–90.9 (3)°) are also a consequence of these longer and more ionic bonds and the smaller spatial requirement of the Tc- - -F_b electron bond pair domain in the valence shell of technetium. Moreover, the F–Tc–F angle (154.9 (3)–155.9 (3)°), which is bent away from the cis oxygen bond pair domains toward the cis fluorine bridges, is very similar to that of WO_2F_2·bpy where the F–W–F angle is 154.8 (3)°.[19]

Although the VSEPR model of molecular geometry[27] accounts for deviations of the cis angles from the ideal 90° angle by attributing them to repulsive interactions between the larger oxygen double bond domains, the model incorrectly predicts that a trans arrangement of oxygens is more stable in this instance. The preference for the cis-oxygen-bonded structure can be understood in terms of the spatial relationship of the strong π-donor oxygen atoms to the approximately $d_{t_{2g}}$ orbitals of technetium required for $p_\pi \rightarrow d_\pi$ bonding and has been noted by Cotton and co-workers[28] for oxomolybdenum species. Moreover, in molybdenum(VI) and tungsten(VI) dioxofluoro compounds, the MO_2 group is not linear and the oxygens assume cis arrangements,[19,29] and it has also been proposed that a greater degree of ligand–metal π-bonding should exist in the case of cis isomers.[29,30] Each oxygen atom of the *cis*-MO_2 groups and the *cis*-TcO_2F_4-unit possesses two filled p-orbitals available for π-bonding with the empty set of metal t_{2g} orbitals. In the trans isomer the two donating p-orbitals on both oxygen atoms compete for the same two $d_{t_{2g}}$ orbitals having the correct symmetry for overlap. In the cis isomer, all three $d_{t_{2g}}$ orbitals are available for overlap. Consequently, the bonding molecular orbitals in the cis isomer have lower energies than the corresponding molecular orbitals in the trans isomer, and the cis isomer should be more stable. It is noteworthy that WO_2F_2·bpy[19] and OsO_2F_4,[31] which has recently been reported, exist exclusively as the *cis*-dioxo isomers, whereas $IO_2F_4^-$ normally exists as a mixture of cis and trans isomers.[32] The exclusive observation of the *cis*-dioxo isomers of OsO_2F_4 and WO_2F_2·bpy is also attributed to $p_\pi \rightarrow d_\pi$ bonding while the cis/trans isomer ratio of $IO_2F_4^-$ is not dominated by $p_\pi \rightarrow d_\pi$ bonding and must be largely kinetically controlled.

A corollary to the dominance of the *cis*-dioxo isomer in dioxofluorometalates having octahedral coordination, and a further consequence of oxygen $p_\pi \rightarrow d_\pi$ bonding is a general tendency for single bonds trans to metal–oxygen double bonds to be longer and therefore weaker. The effect has been specifically noted by Cotton and co-workers[28,33] for single bonds trans to Mo=O double bonds and for several structures in which a fluorine bridge comprises the long bond trans to oxygen, namely, the structure of $MoOF_4$,[17] in which the $MoOF_4$ units are linked by cis-fluorine bridges [Mo- - -F_b, 1.93 (1)–1.96 (1) Å trans to fluorine and 2.27 (1)–2.31 (1) Å trans to oxygen], and for the

(27) Gillespie, R. J.; Hargittai, I. *The VSEPR Model of Molecular Geometry*; Allyn and Bacon, Boston, MA, 1991.
(28) Cotton, F. A.; Morehouse, S. M.; Wood, J. S. *Inorg. Chem.* **1964**, *3*, 1603.
(29) (a) Buslayev, Yu. A.; Kokunov, Yu. V.; Bochkaryova, V. A.; Shustorovich, E. M. *J. Inorg. Nucl. Chem.* **1972**, *34*, 2861 and references therein, (b) Buslaev, Yu. A.; Kokunov, Yu. V.; Bochkareva, V. A.; Shustorovich, E. M. *Russ. J. Inorg. Chem.* (*Engl. Transl.*) **1972**, *17*, 1675 and references therein.
(30) Jaffé, H. H. *J. Phys. Chem.* **1954**, *58*, 185.
(31) Christe, K. O.; Bougon, R. *J. Chem. Soc. Chem. Commun.* **1992**, 1056; private communication.
(32) Christe, K. O.; Wilson, R. D.; Schack, C. J. *Inorg. Chem.* **1981**, *20*, 2104.
(33) Blake, A. B.; Cotton, F. A.; Wood, J. S. *J. Am. Chem. Soc.* **1964**, *86*, 3024.

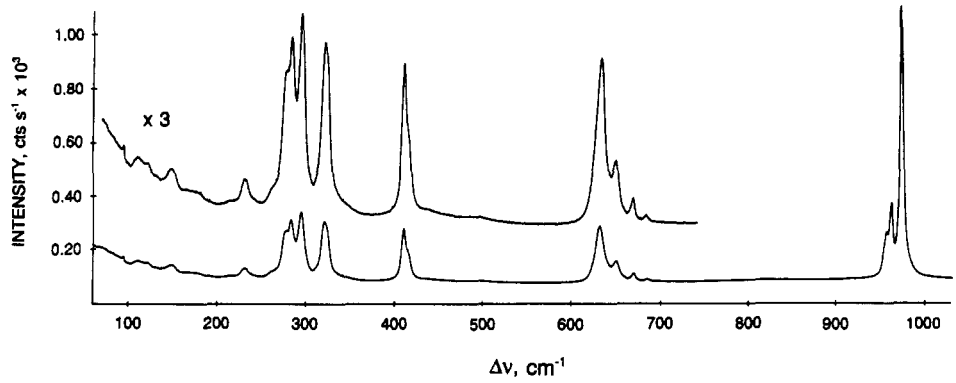

Figure 4. Raman spectrum of microcrystalline TcO_2F_3 recorded in a glass capillary at room temperature using 647.1-nm excitation.

structures of $W_2O_2F_9^-$ [34] and $ReO_2F_9^+$,[34,35] where both W=O and Re=O bonds are trans to the fluorine bridge. Additionally, WO_2F_2·bpy is coordinated with the longer W–N bonds trans to the oxygen atoms,[19] and the MOF_6 units of technetium and rhenium oxotetrafluorides each contain two bridge fluorines, one trans to an oxygen atom and the other trans to a terminal fluorine atom so that, like $MoOF_4$, these structures are also asymmetrically fluorine bridged [Tc- - -F_b, 1.89 (2) Å trans to fluorine and 2.26 (2) Å trans to oxygen;[5] Re- - -F_b, 1.99 (4) Å trans to fluorine and 2.28 (4)–2.31 (4) Å trans to oxygen;[18] the corresponding bond distances in WOF_4 are not compared because the crystal structure presents some inconsistencies, see ref 20]. Spectroscopic studies have also shown that the more ionic metal fluorine (bridge) bonds occur trans to the terminal oxygens in the structures of the $W_2O_2F_9^-$,[36,38] $Mo_2O_2F_9^-$,[39,40] and $MoWO_2F_9^-$ [41] anions and the XeF_2·$n$$MOF_4$,[42,43] and KrF_2·MOF_4[43] (M = Mo or W; n = 1–4) adducts (the noble gas difluoride is coordinated to the metal by means of a fluorine bridge). An X-ray crystal structure has also confirmed that the bridging fluorine atom is trans to the oxygen in XeF_2·WOF_4.[44] In the present study, the crystallographically nonequivalent Tc- - -F_b bonds of the TcO_2F_4 units of TcO_2F_3 are symmetrically fluorine bridged [Tc- - -F_b, 2.048 (1)–2.106 (6) Å; the magnitude of the standard deviations is such that the difference is not significant] with both fluorine bridges trans to oxygen atoms. The Tc- - -F_b bonds are ~0.2 Å shorter than the M- - -F_b bonds trans to oxygen in $MoOF_4$ and $TcOF_4$ and are, in fact, very close to the average of the M- - -F_b bond lengths in these structures. The preference for fluorine bridging trans to oxygens in TcO_2F_3 and related structures appears to be linked to the trans-influence of the doubly bonded oxygens. In addition to the poor π-donor properties of fluorine, the bridging fluorines of these structures must bear more negative charge than their nonbridging counterparts. This charge is reinforced when the strong π-donor oxygen atoms are trans to the fluorine bridges, so that a fluorine trans to oxygen must compete with the oxygen for the same two t_{2g} orbitals, leading to a negligible $p_\pi \rightarrow d_\pi$ contribution from the bridging fluorine and a net build up of negative charge on the bridging fluorine. Because all three $d_{t_{2g}}$ orbitals are available for overlap with fluorine p-orbitals of appropriate symmetry, the terminal fluorines cis to the oxygens are less basic and are not favored for fluorine bridge formation.

Table IV. Raman Frequencies and Assignments for TcO_2F_3[a]

freq, cm^{-1} [b]	assignts for the TcO_2F_4 unit in C_{2v} point symmetry
974 (100)	A_1, $\nu_s(TcO_2)$
963 (27) 958 sh	B_2, $\nu_{as}(TcO_2)$
685 (3) 670 (7)	B_1, $\nu_{as}(TcF_2)_{terminal}$
650 (16) 632 (16)	A_1, $\nu_s(TcF_2)_{terminal}$
416 sh 411 (19)	A_1, $\delta_{sciss}(TcO_2)$
320 (22)	B_2, $\nu_{as}(TcF_2)_{bridge}$
295 (30)	A_1, $\nu_s(TcF_2)_{bridge}$
284 (24)	A_1, $\delta_{sciss}(TcF_2)_{terminal}$
278 sh 264 (2) 231 (3) 215 (<1) 175 (<1) 148 (2) 122 (2) 111 (2)	unassigned deformation modes

[a] The spectrum was recorded on a microcrystalline powder in a Pyrex glass melting point capillary at room temperature using 647.1-nm excitation. [b] Values in parentheses denote relative intensities and sh denotes a shoulder.

Raman Spectroscopy and Vibrational Assignments. Vibrational assignments (Table IV and Figure 4) have been primarily limited to the stretching modes of TcO_2F_3 and are based on the initial assumption that the vibrational modes of the *cis*-TcO_2F_4 unit are weakly coupled allowing assignment under point group C_{2v}. Consequently all 15 vibrational modes having the symmetries $6A_1 + 2A_2 + 3B_1 + 4B_2$ [the [O,O,Tc,F_b,F_b] plane is taken as the $\sigma_v(yz)$-plane with z as the principal axis] are expected to be Raman active. In addition, the asymmetric and symmetric stretching, deformation, and torsional modes associated with the F- - -Tc- - -F bridges are not accounted for in the analysis; however, they would be expected to have low intensities and to occur at very low frequencies and intensities and are unlikely to be easily observed or readily assigned. Although a total of 20 bands are observed, a number of these bands can be attributed to vibrational coupling within the unit cell of TcO_2F_3. In order to evaluate the degree of vibrational coupling, a factor-group analysis of the vibrational modes of the TcO_2F_3 unit cell was carried out by use of the correlation chart method.[45] The symmetry of the free *cis*-TcO_2F_4 unit (C_{2v}) was correlated to the site symmetry (C_1) which corresponds to the site symmetry of the technetium atoms in the unit cell and, in turn, to the crystal

(34) Hoskins, B. F.; Linden, A.; O'Donnell, T. A. *Inorg. Chem.* **1987**, *26*, 2223.
(35) Schrobilgen, G. J.; Holloway, J. H.; Russell, D. R. *J. Chem. Soc., Dalton Trans.* **1984**, 1411.
(36) Darragh, J. I.; Noble, A. M.; Winfield, J. M. *J. Inorg. Nucl. Chem.* **1970**, *32*, 1747.
(37) Buslaev, Yu. A.; Kokunov, Yu. V.; Bochkareva, V. A. *Zh. Strukt. Khim.* **1972**, *13*, 611.
(38) Wilson, W. W.; Christe, K. O. *Inorg. Chem.* **1981**, *20*, 4139.
(39) Buslaev, Yu. A.; Kokunov, Yu. V.; Bochkareva, V. A.; Shustorovich, E. M. *Zh. Strukt. Khim.* **1972**, *13*, 526.
(40) Bueter, A.; Sawodny, W. *Angew. Chem., Int. Ed. Engl.* **1972**, *11*, 1020.
(41) Buslaev, Yu. A.; Kokunov, Yu. V.; Bochkareva, V. A. *Russ. J. Inorg. Chem. (Engl. Transl.)* **1972**, *17*, 1774.
(42) Holloway, J. H.; Schrobilgen, G. J. *Inorg. Chem.* **1980**, *19*, 2632.
(43) Holloway, J. H.; Schrobilgen, G. J. *Inorg. Chem.* **1981**, *20*, 3363.
(44) Tucker, P. A.; Taylor, P. A.; Holloway, J. H.; Russell, D. R. *Acta Crystallogr.* **1975**, *B31*, 906.
(45) Carter, R. L. *J. Chem. Educ.* **1971**, *48*, 297 and references therein.

symmetry (C_i). Assuming complete vibrational coupling occurs within the unit cell of TcO_2F_3, each free molecule mode is expected to be split into two lines having A_g and A_u symmetry in the Raman and infrared spectra, respectively. It is concluded that the *cis*-TcO_2F_4 units are weakly coupled in the Raman spectrum so that several of the assigned modes corresponding to a free *cis*-TcO_2F_4 unit are split into two lines. Consequently, in the assignment of the asymmetric TcO_2 and terminal TcF_2 stretching modes in Table IV, factor-group split bands are listed under the same free molecule symmetry (C_{2v}).

The vibrational assignments for the polymeric *cis*-TcO_2F_4 units in TcO_2F_3 have been guided by the vibrational spectra of *cis*-$IO_2F_4^-$,[32] *cis*-OsO_2F_4,[31] TcO_3F,[6b] and Tc_2O_7.[46] The assignments of the two TcO_2 stretching modes at 958, 963, and at 974 cm^{-1} are straightforward because of their high frequencies and relative intensities. The less intense asymmetric TcO_2 stretch is assigned to a pair of lines (958 and 963 cm^{-1}) to low frequency of its symmetric counterpart at 974 cm^{-1}. This contrasts with the IO_2 stretching modes of *cis*-$IO_2F_4^-$ which have the opposite order (A_1, $\nu_s(IO_2)$, 875 cm^{-1}; B_2, $\nu_{as}(IO_2)$, 856 cm^{-1}). The OsO_2 vibrations in the structurally related *cis*-OsO_2F_4 molecule show the same relative ordering (A_1, $\nu_s(OsO_2)$, 943 cm^{-1}; B_2, $\nu_{as}(OsO_2)$, 933 cm^{-1}) as does TcO_3F with $\nu_{as}(TcO_3)$ at 951 cm^{-1} and $\nu_s(TcO_3)$ at 962 cm^{-1} and Tc_2O_7 with $\nu_{as}(TcO_3)$ at 943 cm^{-1} and $\nu_s(TcO_3)$ at 952 cm^{-1}. It is also characteristic of TcO_3Cl, ReO_3F, ReO_3Cl, and ReO_3Br that the ground-state degenerate asymmetric MO_3 stretching frequency (E) is also observed to be lower than the symmetric one (A_1).[6b,47] The assignments for the terminal TcF stretches are in accord with the TcF stretching frequency of TcO_3F at 696 cm^{-1} and their counterparts in *cis*-$IO_2F_4^-$ (A_1, $\nu_s(IF_2)_{ax}$, 551 cm^{-1}; B_2, $\nu_{as}(IF_2)_{ax}$, 600 cm^{-1}) and *cis*-$OsO_2F_4^-$ (A_1, $\nu_s(OsF_2)_{ax}$, 673 cm^{-1}; B_2, $\nu_{as}(OsF_2)_{ax}$, 680 cm^{-1}). Consequently, A_1, $\nu_s(TcF_2)_{term}$ is assigned to the factor-group split bands at 632 and 650 cm^{-1} and B_1, $\nu_{as}(TcF_2)_{term}$ is assigned to a weaker set of factor-group split bands at 670 and 685 cm^{-1}. Owing to their higher ionic characters (vu = 0.51, Tc- - -F bridge bonds), the TcF_2 bridging stretching frequencies are expected to occur at significantly lower frequencies than the axial TcF_2 stretches (vu = 0.99, Tc–F terminal bonds). The bands at 295 and 320 cm^{-1} are tentatively assigned, based on their relative intensities, to A_1, $\nu_s(TcF_2)_{bridge}$, and B_2, $\nu_{as}(TcF_2)_{bridge}$, respectively. The TcO_2 scissoring deformation is assigned to the factor-group split band at 411 and 416 cm^{-1} by analogy with the A_1, $\delta_{sciss}(MO_2)$ modes of *cis*-$IO_2F_4^-$ (394 cm^{-1}) and *cis*-$OsO_2F_4^-$ (402 cm^{-1}). The assignment of the terminal TcF_2 scissoring deformation and the remaining deformation modes are tentative as no reliable assignments have been published for related *cis*-XO_2F_4 species.

Conclusions

The synthesis of the second known technetium(VII) oxofluoride, TcO_2F_3, is reported for the first time and was achieved by oxide/fluoride metathesis between XeF_6 and Tc_2O_7 in anhydrous HF. The crystal structure of TcO_2F_3 has been determined and is the first structural characterization of a technetium(VII) oxofluoride by diffraction techniques. The structure of TcO_2F_3, like those of $MoOF_4$ and $ReOF_4$, is an open chain polymer in which the oxygen atoms are cis to one another and the TcO_2F_3 units are linked by cis-fluorine bridges which are trans to the oxygen atoms. The coordination about technetium is explained by the spatial relationship of the strong π-donor oxygen atoms to the approximately $d_{t_{2g}}$ orbitals of technetium required for $p_\pi \rightarrow d_\pi$ bonding. The vibrational (Raman) spectrum for TcO_2F_3 is in accord with the X-ray crystal structure and could be assigned to weakly coupled *cis*-TcO_2F_4 units.

Experimental Section

All operations were conducted in laboratories that were monitored routinely by the McMaster University Health Physics Group for radioactive contamination. All work involving ^{99}Tc was performed according to the regulations and recommendations of the Canadian Atomic Energy Control Board.

Apparatus and Materials. All manipulations involving air-sensitive materials were carried out under anhydrous conditions in a drybox or, in the case of volatile fluorides, on a vacuum line constructed of 316 stainless steel, nickel, Teflon, and FEP. All preparative work involving XeF_6 and anhydrous HF was carried out in lengths of $^1/_4$-in. o.d. FEP tubing. The tubing was heat sealed at one end and connected through a 45° SAE flare to a Kel-F valve.

Xenon hexafluoride was prepared using a method similar to that outlined by Chernick and Malm[48] and was ascertained to be free of XeF_4 contaminant using Raman spectroscopy.

Anhydrous HF (Harshaw) was purified using the standard literature method.[49]

Technetium(VII) heptoxide, Tc_2O_7, was prepared by combustion of the metal powder and is a modification of the method described by Selig and Fried.[46] The metal was prepared by reduction of crude $NH_4^+TcO_4^-$ (Oak Ridge National Laboratories) with hydrogen. Crude $NH_4^+TcO_4^-$ (0.294 g) was added to the bottom of a 9-mm o.d. quartz reaction tube through a 6-mm o.d. side tube joined at 90° near the bottom of the reaction tube and heat sealed off under vacuum. The opposite end of the reaction vessel was equipped with a 4-mm Rotaflo glass/Teflon stopcock. Reduction was achieved by initially heating $NH_4^+TcO_4^-$ with a Bunsen flame in the presence of successive aliquots of H_2 followed by removal of H_2O and NH_3 under vacuum. In the latter stages of reduction, the residue was heated to redness with a natural gas–oxygen torch in the presence of each H_2 aliquot and repeated until constant weight was achieved. After further vacuum drying for 24 h, the dry metal was quantitatively converted to Tc_2O_7 by admitting aliquots of dry oxygen gas to the reaction vessel and heating the metal to red heat with a natural gas–oxygen torch until combustion ceased. The Tc_2O_7 that formed condensed as a pale yellow solid in the cooler regions of the silica reactor. The reactor was allowed to cool to room temperature before a second aliquot of dry oxygen gas was admitted. The procedure was repeated until no technetium metal remained. After combustion was complete, the vessel was evacuated and Tc_2O_7 was distilled under static vacuum into the 6-mm o.d. side arm by gently heating the reactor with a Bunsen flame. The side tube was heat sealed off from the reaction tube and transferred to a drybox.

Synthesis of TcO_2F_3 and Crystal Growing. Crystals suitable for X-ray structure determination were obtained by condensing ca. 3 mL of anhydrous HF at −196 °C onto Tc_2O_7 (0.06340 g, 0.2046 mmol) contained in a $^1/_4$-in. o.d., $^1/_{32}$-in. wall thickness FEP tube fitted with a Kel-F valve that had been previously vacuum dried and passivated with fluorine gas. A light yellow layer formed at the bottom of the sample upon warming to room temperature. The mixture was allowed to stand at room temperature for 1 h prior to condensing XeF_6 (0.24858 g, 1.013 mmol) into the sample tube at −196 °C. When the mixture was warmed to room temperature, a bright yellow precipitate formed at the interface of the two phases as the XeF_6 dissolved. The tube and contents were cooled to −78 °C and pressurized to 1000 Torr with dry nitrogen. The sample was warmed to −50 to −55 °C whereupon the yellow solid slowly dissolved to give an equilibrium mixture of $XeF_5^+TcO_2F_4^-$ and XeF_6 in solution (molar ratio XeF_6:Tc_2O_7 = 4.95; see Results and Discussion and eq 9). The tube was allowed to stand inclined at ca. 45° in a 2-L dewar filled with water initially at 55 °C. As the dewar and contents slowly cooled over a day to room temperature, bright yellow parallelepiped-shaped crystals formed which attached to the tube walls. The tube was then cooled to and maintained at 0 °C for several more hours before being cooled to −78 °C and heat sealing off the FEP tube under static vacuum. The sealed tube was maintained at −78 °C and the HF solution was decanted off the crystalline material into the newly sealed tube end. The supernatant was then cooled to −196 °C and the crystalline sample allowed to warm to room temperature so that residual volatiles ($XeOF_4$, trace amounts of XeF_2 and HF) distilled from the sample. The dry crystalline product was isolated from the frozen supernatant by heat sealing. The sample was then transferred to a drybox, the tube was cut open, a Kel-F valve was attached, and the tube was pumped under vacuum at −30 °C to remove any remaining traces of HF and $XeOF_4$. The tube was then transferred to a drybox equipped with a microscope, and the crystals were removed by cutting open the FEP tube and prying them off the walls with a steel needle. The crystals were sealed in Lindemann glass (0.3-mm i.d.) capillaries and stored at −20 °C prior to mounting on the

(46) Selig, H.; Fried, S. *Inorg. Nucl. Chem. Lett.* **1971**, *7*, 315.
(47) Guest, A.; Howard-Lock, H. E.; Lock, C. J. L. *J. Mol. Spectrosc.* **1978**, *72*, 143.
(48) Malm, J. G.; Chernick, C. L. *Inorg. Synth.* **1966**, *8*, 258.
(49) Emara, A. A. A.; Schrobilgen, G. J. *Inorg. Chem.* **1992**, *31*, 1323.

diffractometer. A preliminary observation of the sealed crystals under a polarizing microscope revealed that all of them were single. The crystal used in this study had the following dimensions: 0.3 × 0.3 × 0.625 mm. Following X-ray data collection, the Raman spectrum of the single crystal was obtained and shown to be identical to the bulk sample (see Table IV and Figure 4).

A second preparation of TcO_2F_3 was carried out in the manner described above (Tc_2O_7, 0.13324 g, 0.43007 mmol; XeF_6, 0.34232 g, 1.39563 mmol; HF 3 mL) except that the yellow precipitate of TcO_2F_3 was only slightly soluble in HF owing to the use of an amount of XeF_6 in slight excess of the ideal 3:1 stoichiometry (molar ratio XeF_6:Tc_2O_7 = 3.24; see Results and Discussion and eqs 1–3 and 6) and could not be crystallized from HF. Rather, after the FEP reaction tube was heat sealed off near the valve, the supernatant consisting of HF, $XeF_5^+TcO_2F_4^-$, $XeOF_4$, and a trace of XeF_2 was decanted into the other end of the tube and the solid TcO_2F_3 washed free of small amounts of $XeF_5^+TcO_2F_4^-$ by chilling the tube end containing the solid so that HF (and $XeOF_4$) back distilled onto the solid. After resuspending, allowing the powder to settle, and decanting, we repeated the decantation/back distillation cycle two more times before the powdered sample was isolated as described previously for the crystallographic sample of TcO_2F_3 (yield 92%).

In both preparations, small amounts of O_2 gas were liberated that are attributable to reactions (4) and (5).

Crystal Structure Determination of TcO_2F_3. Collection and Reduction of X-ray Data. The crystal was centered on a Syntex $P2_1$ diffractometer. Examination of the peak profiles revealed they were slightly broadened but single. Accurate cell dimensions were determined at $T = -100$ °C from a least-squares refinement of the setting angles (χ, ϕ, and 2θ) obtained from 21 accurately centered reflections (with $13.92° \le 2\theta \le 29.76°$) chosen from a variety of points in reciprocal space. Integrated diffraction intensities were collected using a θ–2θ scan technique with scan rates varying from 1.5 to 14.65°/min (in 2θ) and a scan range of ±0.6° so that the weaker reflections were examined most slowly to minimize counting errors. The data were collected in two steps. In a first step, they were collected with $0 \le h \le +9$, $-9 \le k \le +9$, and $-14 \le l \le +14$ and $3 \le 2\theta \le 40°$ using silver radiation monochromatized with a graphite crystal ($\lambda = 0.56086$ Å). During data collection, the intensities of three standard reflections were monitored every 97 reflections to check for crystal stability and alignment. A total of 2979 reflections were collected out of which 69 were standard reflections. In a second step, the data were collected with $0 \le h \le +11$, $-11 \le k \le +11$, and $-17 \le l \le +17$ and $40 \le 2\theta \le 50°$. A total of 4911 unique reflections remained after averaging of equivalent reflections of which 2093 satisfied the condition $I \ge 3\sigma(I)$ and were used for structure solution. No decay was observed. An empirical absorption correction was applied to the data by using the ϕ scan method ($\Delta\phi = 10°$) ($\mu R = 2.622$). Corrections were made for Lorentz and polarization effects.

Crystal Data. The compound TcO_2F_3 (fw = 187.0 g mol^{-1}), crystallizes in the triclinic system, space group $P\bar{1}$, with $a = 7.774$ (3) Å, $b = 7.797$ (1) Å, $c = 11.602$ (3) Å, $\alpha = 89.41$ (2)°, $\beta = 88.63$ (3)°, $\gamma = 84.32$ (2)°, $V = 699.6$ (3) Å^3, and $D_{calc} = 3.551$ g cm^{-3} for $Z = 8$. Ag(Kα) radiation ($\lambda = 0.560\,86$ Å, μ(Ag Kα) = 128.42 cm^{-1}) was used.

Solution and Refinement of the Structure. The XPREP program[50] was used for determining the correct cell and space group and first confirmed the original cell and that the lattice was triclinic primitive ($R_{int} = 0.022$). The structure was shown to be centrosymmetric by an examination of the E-statistics (calculated, 1.079; theoretical, 0.968), and consequently the structure was solved in the space group $P\bar{1}$.

A first solution was obtained without absorption corrections and it was achieved by direct methods which located the positions of the technetium atoms. The full-matrix least-squares refinement of the technetium atom positions and isotropic thermal parameters gave a conventional agreement index R ($=\Sigma||F_o| - |F_c||/\Sigma|F_o|$) of 0.20. A difference Fourier synthesis revealed the remaining fluorine and oxygen atoms and confirmed the presence of TcO_2F_3 in a polymeric form. Two of the fluorines appeared to be on special positions (they happened to be bridging fluorines), while all the other F and O atoms occupied general positions. Refinement of positional and isotropic temperature parameters for all atoms (the oxygen atoms being assigned a fluorine scattering factor) converged at $R = 0.11$. At this stage, it was possible to distinguish, in each technetium environment, two bond lengths which were significantly shorter than the other ones, indicating the presence of two Tc–O double bonds. A significant improvement of the structure was achieved by introducing anisotropic thermal parameters for the O and F atoms, reducing R to 0.056.

(50) Sheldrick, G. M. *SHELXTL PLUS*, Release 4.21/V; Siemens Analytical X-Ray Instruments, Inc.: Madison, WI, 1990.

The structure was solved a second time using data that had been corrected empirically for absorption, and this time all of the F and O atoms were refined with anisotropic thermal parameters ($R = 0.050$). The final refinement was obtained by introducing a weight factor ($w = 1/\sigma^2(F) + 0.008686F^2$) and gave rise to a residual, R, of 0.042 ($R_w = 0.043$). In the final difference Fourier map, the maximum and the minimum electron densities were +1.97 and –0.94 eÅ^3.

All calculations were performed on a 486 personal computer using the SHELXTL PLUS[50] determination package for structure solution and refinement as well as structure determination molecular graphics.

Nuclear Magnetic Resonance Spectroscopy. All spectra were recorded unlocked (field drift < 0.1 Hz h^{-1}) on a Bruker AM-500 spectrometer equipped with an 11.744-T cryomagnet and an Aspect 3000 computer. The spectra were obtained using a 10-mm broad-band VSP probe (tunable over the range 23–202 MHz), which was tuned to 104.631 and 139.051 MHz to observe ^{99}Tc and ^{129}Xe, respectively. Fluorine-19 spectra were obtained by retuning the ^{1}H-decoupling coil of the probe to the fluorine frequency, 470.600 MHz. Free induction decays for ^{19}F and ^{99}Tc were accumulated in 16K memory with spectral width settings of 10 and 50 kHz, respectively, yielding acquisition times of 0.819 and 0.164 s and data point resolutions of 1.2 and 6.1 Hz/data point, respectively. Free induction decays for ^{129}Xe were accumulated in 32K memories with spectral width settings of 100 kHz and yielded an acquisition time of 0.164 s and data point resolution of 6.1 Hz/data point, respectively. No relaxation delays were applied. Typically, 2000–10000 transients were accumulated for ^{99}Tc and ^{129}Xe spectra and 1000 for ^{19}F spectra. The pulse widths corresponding to a bulk magnetization tip angle, θ, of approximately 90° were 1 μs (^{19}F), 14 μs (^{99}Tc), and 18 μs (^{129}Xe). Line broadening parameters used in the exponential multiplication of the free induction decays were 4 Hz in the ^{19}F spectra, 10 Hz in the ^{99}Tc spectra, and 20–30 Hz in the ^{129}Xe spectra.

The ^{19}F, ^{99}Tc, and ^{129}Xe NMR spectra were referenced to external samples of neat $CFCl_3$, 0.210 M aqueous $NH_4^+TcO_4^-$, and neat $XeOF_4$, respectively, at 30 °C. The chemical shift convention used is that a positive (negative) sign indicates a chemical shift to high (low) frequency of the reference compound.

The NMR spectra of the supernatants (see Results and Discussion) were obtained at 30 °C by inserting a sealed $^1/_4$-in. o.d. FEP plastic tube end containing a supernatant into a thin-walled glass precision NMR tube (Wilmad) and spinning in the probe.

Raman Spectroscopy. Raman spectra were recorded on an Jobin-Yvon Mole S-3000 triple spectrograph system equipped with a 0.32-m prefilter, adjustable 25-mm entrance slit, and a 1.00-m monochromator. Holographic gratings were used for the prefilter (600 grooves mm^{-1}, blazed at 500 nm) and monochromator (1800 grooves mm^{-1}, blazed at 550 nm) stages. An Olympus metallurgical microscope (model BHSM-L-2) was used for focusing the excitation laser to a 1-μm spot on the sample. The 647.1-nm line of a Kr ion laser was used for excitation of the sample. Spectra were recorded at ambient temperature on a powdered microcrystalline sample sealed in a baked-out Pyrex melting point capillary as well as on the single crystal used to determine the X-ray structure sealed in its original glass Lindemann capillary. The spectra were recorded by signal averaging using a Spectraview-2D CCD detector equipped with a 25-mm chip (1152 × 298 pixels) and at a laser power of 20 MW at the sample and slit settings corresponding to a resolution of 1 cm^{-1}. A total of 10 reads having 30-s integration times were summed. Spectral line positions are estimated to be accurate to ≅ 1 cm^{-1}.

Acknowledgments. We thank the U.S. Air Force Phillips Laboratory, Edwards Air Force Base, CA, for support of this work under Contract F04611-91-K-0004 and the National Sciences and Engineering Research Council of Canada for support in the form of an operating grant. The authors also thank Prof. Neil Bartlett for his helpful discussions relating to the X-ray crystal structure and Drs. Karl O. Christe and Roland Bougon for making available to us their vibrational assignments for *cis*-OsO_2F_4 prior to publication.

Supplementary Material Available: A structure determination summary (Table 5), a table of anisotropic thermal parameters (Table 6), a table of intermolecular and intramolecular contacts less than 3.5 Å (Table 7), and an ORTEP stereoview of the packing in the unit cell (Figure 5) (7 pages). Ordering information is given on any current masthead page.